Quaternary Science Reviews 106 (2014) 316–329

Contents lists available at ScienceDirect

Quaternary Science Reviews

journal homepage: www.elsevier.com/locate/quascirev

Past circulation along the western Iberian margin: a time slice vision from the Last Glacial to the Holocene

E. Salgueiro [a, b, *], F. Naughton [a, b], A.H.L. Voelker [a, b], L. de Abreu [c], A. Alberto [a], L. Rossignol [d], J. Duprat [d], V.H. Magalhães [a, d], S. Vaqueiro [c], J.-L. Turon [e], F. Abrantes [a, b]

[a] Divisão de Geologia e Georecursos Marinhos, Instituto Português do Mar e da Atmosfera (IPMA), Lisboa, Portugal
[b] CIMAR Associate Laboratory, CIIMAR, Porto, Portugal
[c] IPMA Collaborator
[d] Instituto Dom Luiz (LA), Portugal
[e] UMR-CNRS 5805 EPOC, Université de Bordeaux, Allée Geoffroy St Hilaire, 33615 Pessac, France

ARTICLE INFO

Article history:
Received 16 February 2014
Received in revised form
20 July 2014
Accepted 2 September 2014
Available online 23 September 2014

Keywords:
Paleotemperature
Paleoproductivity
Iberian margin
Last Glacial Maximum
Heinrich stadial
Younger Dryas
Planktonic foraminifera

ABSTRACT

Fifteen Iberian margin sediment cores, distributed between 43°12′N and 35°53′N, have been used to reconstruct spatial and temporal (sub)surface circulation along the Iberian margin since the Last Glacial period. Time-slice maps of planktonic foraminiferal derived summer sea surface temperature (SST) and export productivity (Pexp) were established for specific time intervals within the last 35 ky: the Holocene (Recent and last 8 ky), Younger Dryas (YD), Heinrich Stadials (HS) 1, 2a, 2b, 3, and the Last Glacial Maximum (LGM). The SST during the Holocene shows the same latitudinal gradient along the western Iberian margin as present-day with cold but productive areas that reflect the influence of coastal upwelling centers. The LGM appears as a slightly less warm, but more productive period relative to the Holocene and present-day conditions, suggesting that sea-level minima forced a westward displacement of the coastal upwelling centers possibly accompanied by a strengthening of northward winds. During the YD, a longitudinal thermal front is depicted at 10°W, with cold polar waters offshore and warmer subtropical waters inshore, suggesting that the subtropical Paleo-Iberian Poleward Current more likely flowed at a more inshore location masking the local SST signal and amplitude of variation. A substantial cooling and drop in productivity is observed during all HS, in particular HS1 and HS3, reflecting the penetration of icebergs-derived meltwater. These most extreme southward extensions of very cold waters define a strong SST gradient that marks a possible Paleo-Azores Front. Higher production south of this front was likely fed by frontal nutrient advection.

1. Introduction

Coastal upwelling regions are considered areas of significant biological productivity in Eastern Boundary Current Systems, representing 80–90% of the new production (e.g., Hill et al., 1998). These areas are considered as key locations to understand the linkage between the biological pump, or export productivity and climate in the past, which is essential for simulating future climate. The western Iberian margin is part of the Canary Current related upwelling system with centers of highest productivity located off Cape Finisterre in the north and off Cape St. Vicente in the south.

In the past, the Iberian Margin has experienced drastic changes in hydrography and associated productivity. Due to the southward displacement of the Polar Front, melting icebergs and subpolar waters reached the Iberian margin during the Greenland stadials (GS) of the Last Glacial, including Heinrich stadials (HS) and the Younger Dryas (YD) (Cayre et al., 1999; Bard et al., 2000; de Abreu et al., 2003; Eynaud et al., 2009). Along the western Iberian margin, surface waters cooled during stadials at least by 5 °C, with HS showing largest sea surface temperature (SST) drops (de Abreu et al., 2003; Martrat et al., 2007; Eynaud et al., 2009; Naughton et al., 2009; Salgueiro et al., 2010). The intensity of the cooling, however, declined southwards due to the increasing influence of subtropical waters (Salgueiro et al., 2010; Voelker and de Abreu, 2011). In the Gulf of Cadiz, cold surface water episodes were restricted to HS (Voelker et al., 2009; Voelker and de Abreu, 2011). During the Last Glacial Maximum (LGM), a period relatively warm

* Corresponding author. Divisão de Geologia e Georecursos Marinhos, Instituto Português do Mar e da Atmosfera (IPMA), Lisboa, Portugal.
E-mail addresses: emilia.salgueiro@lneg.pt, emilia.salgueiro@ipma.pt (E. Salgueiro).

http://dx.doi.org/10.1016/j.quascirev.2014.09.001
0277-3791/

compared to the surrounding HS (Eynaud et al., 2009; Voelker et al., 2009; Salgueiro et al., 2010; Penaud et al., 2011) productivity increased significantly within this upwelling system, both along the Iberian and NW African margins, possibly associated to stronger westerly winds (Abrantes, 1991, 1992; Lebreiro et al., 1997; Kohfeld et al., 2005; Eberwein and Mackensen, 2008; Romero et al., 2008). Using core transects along the Portuguese margin, Voelker et al. (2009) and Salgueiro et al. (2010) showed that productivity varied in response to millennial-scale climate oscillations. A decrease in productivity during GS and HS is recorded north of 39–40°N, whereas most records from the Sines margin (Fig. 1a) show a complex signal (Salgueiro et al., 2010). In the Gulf of Cadiz, on the other hand, enhanced productivity is observed during GS, including HS1 and the YD (GS1) (Voelker et al., 2009; Penaud et al., 2010, 2011). This higher glacial productivity was related to the presence of nutrient-rich waters associated with the eastward extension of the Azores Front into the Gulf of Cadiz (Voelker et al., 2009; Penaud et al., 2011).

Most of the hydrography and productivity studies were concentrated on variations in time. Understanding spatial variability of paleo-data is, however, crucial for a comparison with climate model results (e.g., Schmittner, 2005; Kageyama et al., 2010) as well

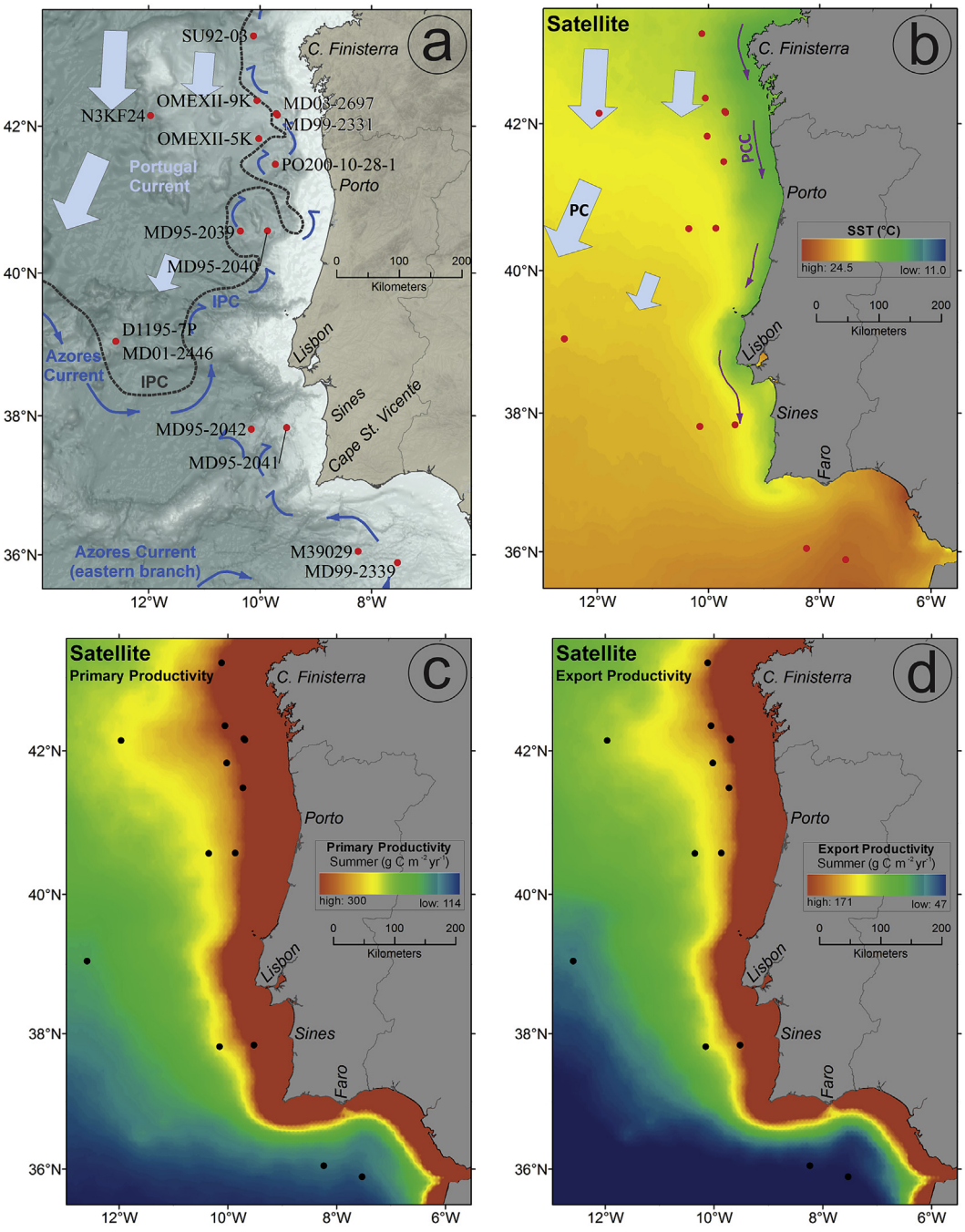

Fig. 1. Modern oceanographic conditions: a) location of the 15 sediment cores used in this study, and winter superficial currents; b) satellite summer derived sea surface temperature (SST), and summer superficial currents; c) summer satellite derived primary productivity (PP) d) summer exported productivity (Pexp) calculated from summer PP. All satellite data were downloaded from Ocean productivity site from Oregon State University (http://www.science.oregonstate.edu/ocean.productivity; Behrenfeld and Falkowski, 1997).

as for a better knowledge of the impact of abrupt climate events on ocean productivity (Mariotti et al., 2012). Few regions in the world have been as densely cored as the Iberian margin. Here, we use published and unpublished data from 15 cores (Fig. 1a) to map spatial and temporal gradients in hydrography and productivity along the margin. We focus on seven time slices over the last 35 ky, including the Holocene, the LGM, YD, and HSs.

2. Oceanographic settings

The western Iberian margin is characterized by seasonal (May to September) coastal upwelling triggered by enhanced northerly winds as supported by the presence of cold and nutrient-rich Eastern North Atlantic Central Waters (ENACW) close to the coast. During upwelling regimes, filaments and plumes (off the capes) penetrate more than 200 km offshore into the open ocean along most of the western Iberian margin, but the filaments off Cape Finisterra and Cape St. Vicente are the most persistent (Fiúza, 1984; Haynes et al., 1993; Fiúza et al., 1998). Off Cape St. Vicente, filaments flow first around the cape, and then further to the east, over the shelf on the southwestern coast (e.g., Fiúza et al., 1982; Relvas and Barton, 2002), where upwelling can occasionally occur when westerly winds locally blow (Fiúza, 1983; Relvas and Barton, 2002). ENACW, with a subtropical (ENACWst) or a subpolar (ENACWsp) origin, is the source of the upwelled water. Depending on wind strength, either type of ENACW can be upwelled. North of Lisbon, however, the importance of the subtropical branch decreases. ENACWst, formed by strong evaporation and winter cooling along the Azores Front (Fiúza, 1984; Rios et al., 1992), is relatively warmer and saltier and contains less nutrients than the ENACWsp's southward flowing branch. Denser ENACWsp occurs below subtropical ENACWst, and is formed in the eastern North Atlantic at 46°N (Fiúza, 1984; Rios et al., 1992; Fiúza et al., 1998).

During coastal upwelling events, surface ocean circulation is characterized by the southward recirculation of the North Atlantic Drift, i.e. the Portugal Current flowing in the open ocean west of 10°W (Peliz et al., 2005), and the Portugal Coastal Current, close to the western Iberian coast, and responsible for the southward transport of the upwelled waters (Fiúza, 1984; Alvarez-Salgado et al., 2003; Peliz et al., 2005, Fig.1b). During winter, the Portugal Coastal Current is replaced by the northward subtropical Iberian Poleward Current, a slope current derived from the Azores Current (Fiúza, 1984; Fiúza et al., 1998; Peliz et al., 2005, Fig. 1a). The Azores Current, which is another branch of the North Atlantic Drift, flows into the Gulf of Cadiz and contributes to the formation of the subtropical front (Azores Front) around 36°N (Peliz et al., 2005). During winter, changes in wind regimes and increases in meridional density gradients of the slope waters (e.g., Frouin et al., 1990) cause Azores Current waters to recirculate from the Gulf of Cadiz around Cape St. Vicente to the southwest Iberian margin. Around 39°N, the Iberian Poleward Current shifts from an eastward to a northward flow direction, following the Iberian margin into the Bay of Biscay during winter and thereby contributing to a predominant feature: the Western Iberia Winter Front (Frouin et al., 1990; Peliz et al., 2005). The Iberian Poleward Current's subsurface component is the ENACWst (e.g., Frouin et al., 1990), while the Portugal Current's subsurface component is the ENACWsp (e.g., Perez et al., 2001).

3. Material and methods

To understand the behavior of the western Iberian upwelling system under different paleoclimate baseline conditions, we compiled planktonic foraminifera $\delta^{18}O$ records and the relative abundance data of planktonic foraminifera of fifteen deep-sea sediment cores (SU92-03, OMEXII-9K, N3KF24, MD03-2697, MD99-2331, OMEXII-5K, PO200/10-28-1, MD95-2039, MD95-2040, D1195-7P, MD01-2446, MD95-2041, MD95-2042, M39029-7, MD99-2339), distributed along the Iberian margin between 43°12′N and 35°53′N (Fig. 1a, Table 1) and covering the last 35 ky BP (Kilo years before present). The geographical and temporal coverage allows mapping summer sea surface temperature (SST) and export productivity (Pexp) patterns and, in particular, identifying the most productive areas along the Iberian margin under different climatic and oceanographic contexts.

3.1. Chronostratigraphy

We used the published age models of cores SU92-03, MD03-2697, MD99-2331, MD95-2039, MD95-2040, MD01-2446, MD95-2042, M39029-7 and MD99-2339, which have been reconstructed based on calibrated Accelerator Mass Spectrometry ^{14}C ages and on the correlation of the *Globigerina bulloides* $\delta^{18}O$ signal to the GISP2 $\delta^{18}O$ record (Table 1). Two different age models have been published for cores MD03-2697 and MD99-2331 (Naughton et al., 2007; Sanchez-Goni et al., 2008). One is based on calibrated ^{14}C ages (Naughton et al., 2007, 2009) while the second one is based on ^{14}C ages back to 26 ka and the isotopic tuning to core MD95-2042 from 26 ky downwards, which chronology was obtained by peak-to-peak correlation of the *G. bulloides* $\delta^{18}O$ with the GISP2 $\delta^{18}O$ record (Bard et al., 2004; Sanchez-Goni et al., 2008). In this paper, we use the Sanchez-Goni et al. (2008) age model.

Chronology for the remaining cores is based on calibrated ^{14}C ages combined with foraminiferal $\delta^{18}O$ tuning to the SPECMAP (Imbrie et al., 1984; Martinson et al., 1987) or GISP2 ice-core $\delta^{18}O$ records, and/or comparing *G. bulloides* $\delta^{18}O$ and % *Neogloboquadrina pachyderma* (sinistral) with the respective high-resolution (~150 years) records of core MD95-2040 (itself partially tuned to GISP2; de Abreu et al., 2003; Salgueiro et al., 2010). Another approach was the alignment of limits for specific events (such as HS) on the basis of other proxy indicators like abundance of detrital grains and relative abundance of *N. pachyderma* (sinistral) (Shacketon, 2000; de Abreu, 2000; Schönfeld et al., 2003; de Abreu et al., 2003; Voelker et al., 2006; Eynaud et al., 2009; Naughton et al., 2009; Salgueiro et al., 2010; Alberto, 2012). The age model of core MD95-2041 is a combination of the one published by Voelker et al. (2009) and tuning of *G. bulloides* $\delta^{18}O$ and percentages of *N. pachyderma* (sinistral) records to those of core MD95-2040 (Figs. 2 and 3). Age models of cores PO200-10-28-1 and OMEXII-9K are based on calibrated ^{14}C ages, according to Abrantes et al. (1998) and Hall and McCave (2000), respectively. However, we adjusted both age models by aligning *G. bulloides* $\delta^{18}O$ and *N. pachyderma* (sinistral) signals with those recorded in core MD95-2040 during HS2a,b and HS3 (Figs. 2 and 3). Age models of low-resolution cores OMEXII-5K, N3KF24 and D11957P were established by tuning the *G. bulloides* $\delta^{18}O$ data and *N. pachyderma* (sinistral) percentage maxima with the respective records of core MD95-2040. This correlation takes into account sedimentation rates obtained for the primarily published stratigraphies, i.e. de Abreu (2000) for OMEXII-5K and N3KF24; Lebreiro et al. (1997) and de Abreu (2000) for D11957P (Figs. 2 and 3).

All data presented in this paper will be available on the PANGAEA data server (www.pangaea.de).

3.2. Temperature and productivity reconstructions

Summer SST and Pexp were reconstructed based on the planktonic foraminifera assemblages found within the >150 μm sediment fraction and modern analog databases. For the present-day SST database, now extended to 1066 core tops, SST of 10 m water

Table 1
Detailed information on the studied cores.

Core	Cruise	Latitude (°N)	Longitude (°W)	$\delta^{18}O$ *G. bulloides*	Plank foram. counts	Age model	AMS^{14}C
SU92-03	PALEOCINAT II (1992)	43.196	10.113	Salgueiro et al. (2010)	Salgueiro et al. (2010)	Salgueiro et al. (2010)	Yes
OMEXII-9K	OMEX II (1997)	42.343	10.051	Hall and McCave 2000	This study	Hall and McCave 2000; This study	Yes
N3KF24	NORESTLANTE III (1989)	42.141	11.959	de Abreu (2000)	de Abreu (1995)	de Abreu (2000); This study	No
MD03-2697	MD134/PICABIA (2003)	42.166	9.703	Naughton et al. (2007)	Naughton et al. (2007)	Naughton et al. (2007)	Yes
MD99-2331	MD114/IMAGES V (1999)	42.150	9.683	Naughton et al. (2007)	Naughton et al. (2007)	Naughton et al. (2007, 2009); Sanchez Goñi et al., 2008	Yes
OMEXII-5K	OMEX II (1997)	41.833	10.018	de Abreu (2000)	de Abreu (2000)	de Abreu (2000); This study	No
PO200-10-28-1	PO200/10 (1993)	41.488	9.722	Abrantes et al. (1998)	Abrantes et al. (1998)	Abrantes et al. (1998); This study	Yes
MD95-2040	MD101/IMAGES I (1995)	40.582	9.862	de Abreu et al. (2000, 2003); Schönfeld et al. (2003)	de Abreu et al. (2000, 2003); Schönfeld et al. (2003)	de Abreu et al. (2000, 2003); Salgueiro et al. (2010)	Yes
MD95-2039	MD101/IMAGES I (1995)	40.578	10.348	de Abreu (2000); Schönfeld et al. (2003)	de Abreu (2000); Schönfeld et al. (2003)	de Abreu (2000); Schönfeld et al. (2003); Eynaud et al. (2009)	Yes
D11957P	Discovery 187 (1989)	39.050	12.583	Lebreiro et al. (1997)	Lebreiro et al. (1997)	Lebreiro et al. (1997); This study	No
MD01-2446	VT100/AMOCINT INETI (2008)	39.056	12.624	–	Alberto (2012)	Alberto (2012)	Yes
MD95-2042	MD101/IMAGES I (1995)	37.811	10.150	Shackleton (2000)	Chabaud et al., submitted to The Holocene	Shackleton (2000); Salgueiro et al. (2010)	Yes
MD95-2041	MD101/IMAGES I (1995)	37.833	9.518	Voelker et al. (2009) Voelker and de Abreu (2011)	Voelker et al. (2009) Voelker and de Abreu (2011)	Voelker et al. (2009), and tuning to MD95-2040 for age >30 ky	Yes
M39029-7	Cruise M-39 (1996)	36.050	8.233	(Loewemark, 2001)	Reguera (2001)	Colmenero-Hidalgo et al. (2004)	Yes
MD99-2339	MD114/IMAGES V (1999)	35.886	7.528	Voelker et al. (2006)	Voelker et al. (2006, 2009) Voelker and de Abreu (2011)	Voelker et al. (2006)	No

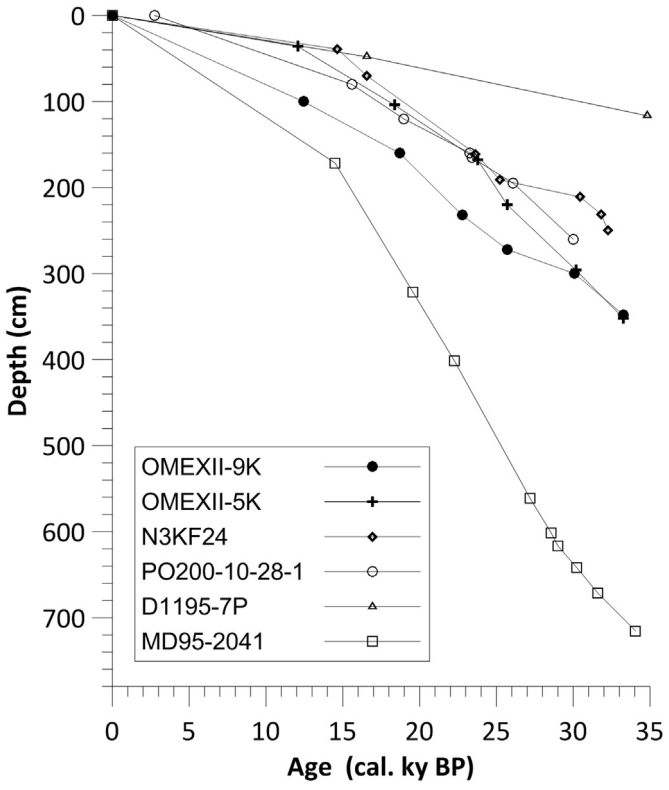

Fig. 2. $\delta^{18}O$ *G. bulloides* (‰VPDB) and % *N. pachyderma* (sinistral) records for the 15 sediment cores used in this study, and their correlation with the GISP2 Greenland ice core $\delta^{18}O$ records (Stuiver and Grootes, 2000).

depth was retrieved from the World Ocean Atlas (WOA) 1998. The present-day productivity database, now with 1039 top-cores, is based on the oceanic primary productivity deducted from satellite color data (8 year averages; Antoine et al., 1996) and converted into Pexp following the published empirical equations (Eppley and Peterson, 1979; Sarnthein and Winn, 1988). The former calibrations display high correlation coefficients between estimated and measured SST and Pexp of 0.995 and 0.9, respectively (Salgueiro et al., 2010). The improved SST and Pexp modern analog database includes indeed new core top data from regions with strong temperature and productivity gradients due to upwelling cells off NW Galicia and off NW Africa. The additional sites should help minimizing no- or less-analog conditions observed with the regional (Salgueiro et al., 2008) and North Atlantic calibrations (Salgueiro et al., 2010). We calculated past SST and Pexp using the SIMMAX non-distance-weighted option (SIMMAX ndw), similar to the classical MAT technique, to estimate more realistic and robust SST values (Telford et al., 2004).

The Holocene and Recent SST and Pexp reconstructions will be compared with high temporal (12 year average) and spatial resolution satellite data (R. O'Malley and M. Behrenfeld, personal communication; http://www.science.oregonstate.edu/ocean.productivity/; Behrenfeld and Falkowski, 1997, Fig. 1b–d). Pexp was derived from primary productivity calculations that include MODIS surface chlorophyll concentrations, SST and photosynthetically active radiation. Datasets are available at 8-day interval with a spatial resolution of 9 km. For this reason, the data interpolated from this database at each site allows to better identify the present-day oceanographic features of the region than the Antoine et al. (1996) data (Supplementary Fig. 1). However, both databases show the same pattern and are correlated (Supplementary Figs. 1 and 2), just as are satellite SST and WOA 1998 data (Supplementary Fig.3).

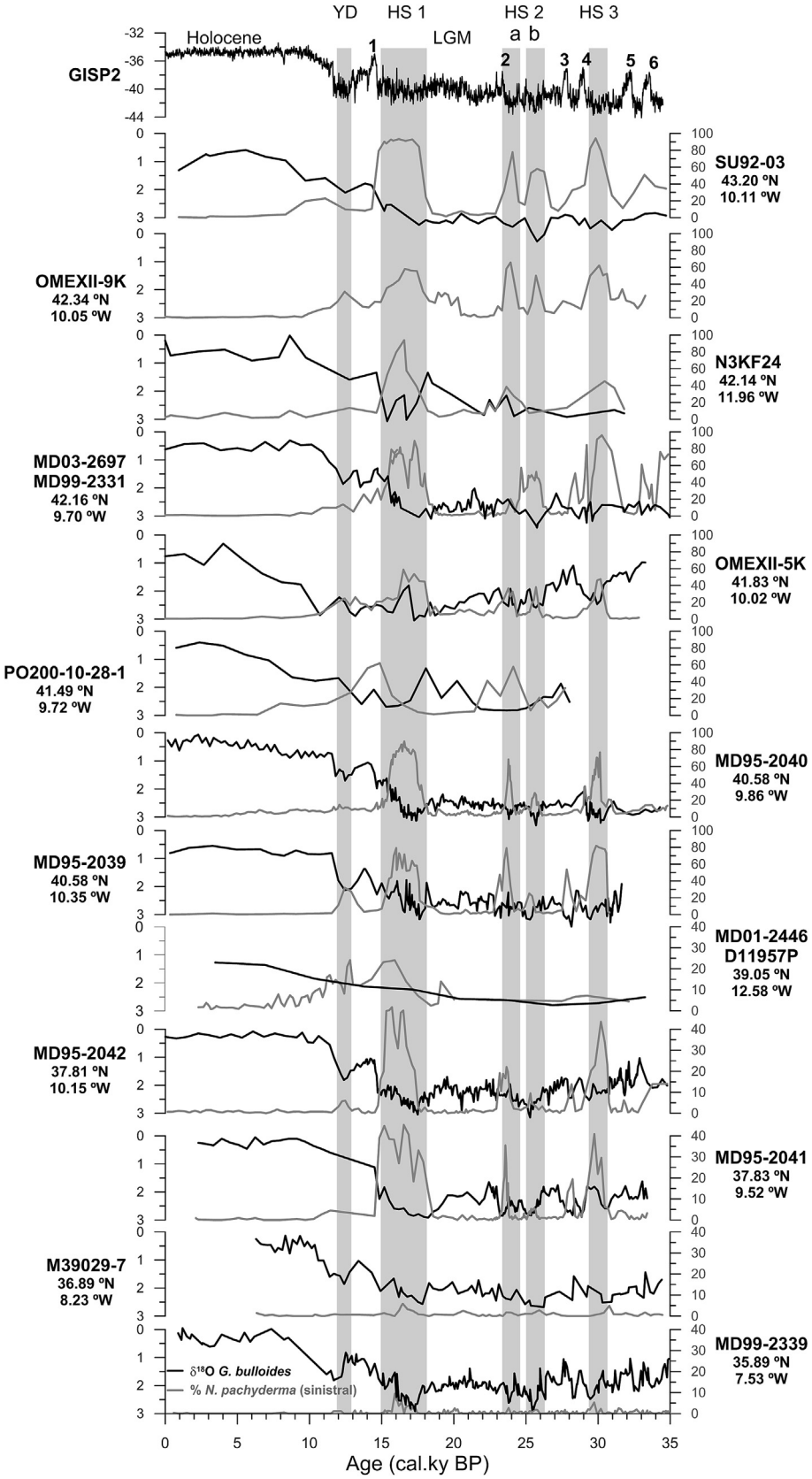

Fig. 3. Age versus depth plots for cores: OMEXII-9K; N3KF24; OMEXII-5K; PO200-10-28-1; D11957P; and MD95-2041.

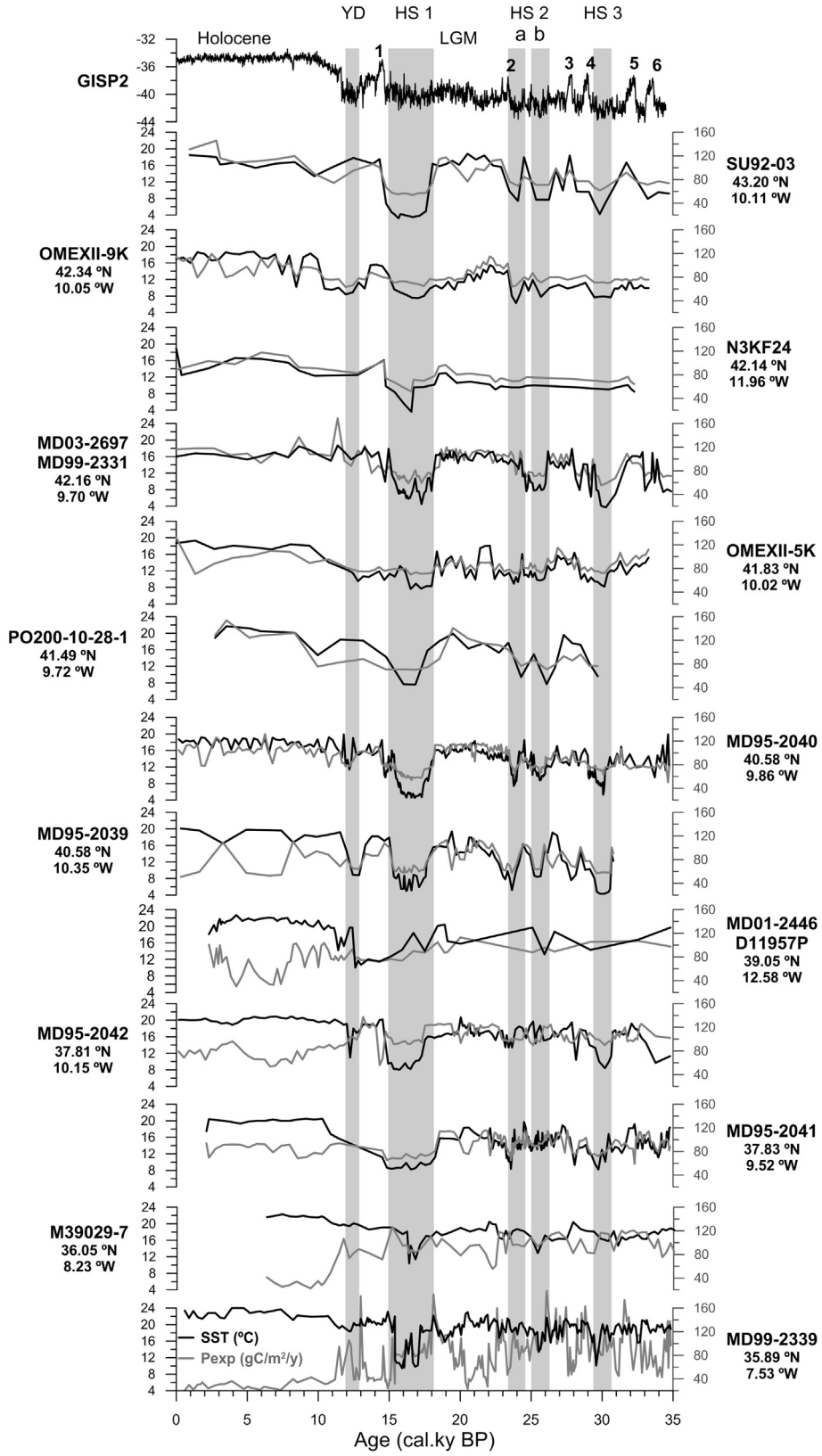

Fig. 4. Summer sea surface temperature (SST) (°C) and export productivity (Pexp) (gC/m^2/y) records for the 15 sediment cores used in this study, and their correlation with the GISP2 Greenland ice core $\delta^{18}O$ record (Stuiver and Grootes, 2000).

3.3. Temperature and productivity mapping

SST and Pexp reconstructions of each site and time interval, within the age boundaries defined for each time-slice, were averaged in order to capture the mean state reaction to major climate changes (Supplementary Table 1). Modern SST and Pexp conditions in Fig. 5 were mapped for each core's position using the values of the higher resolution satellite data (R. O'Malley and M. Behrenfeld, personal communication; Fig. 1) with the satellite PP converted to Pexp the same way as the Antoine et al. (1996) data (see Section 3.2).

3.3.1. Holocene

The Holocene reconstruction is represented by two maps: 1) the Recent time slice and 2) the longer term Holocene. The Recent time slice, based on the core-top samples with ages $\leq$1000 years, is used for validating our approach as it reveals differences and similarities to the present-day SST and Pexp conditions (i.e., modern satellite data). For the Holocene per se, SST and Pexp values were averaged over the last 8.000 years in order to avoid changes related to the 8.2 ka cold event (Holocene <8 ky; Fig. 3).

3.3.2. Last Glacial Maximum

Although the maximum extension of Northern Hemisphere ice sheets and minimum sea-level occurred between 30 and 19 ka (Lambeck et al., 2002), this interval was punctuated by a number of GS/Greenland interstadials (GI), including HS. The LGM has been identified as the interval between HS2 and HS1 when the warming of GI 2 was undetectable (e.g., Elliot et al., 1998; Naughton et al., 2007). That is, between 23 and 19 ka to avoid the GI 2 event in several regions (Mix et al., 2001), or between 21 and 19 ka interval, if based on the complex SST signal recorded along the Iberian margin (Voelker et al., 2009). Here, we follow Voelker et al. (2009) and use the 21 to 19 ka interval for the LGM time slice.

3.3.3. Younger Dryas

Since this particular cold event is not detectable in every Iberian margin record, we have used the highest time resolution records for delimiting the YD. Age limits of 12.9 to 11.8 ka BP (Fig. 3) are in agreement with those proposed for the YD in the Iberian margin (Naughton et al., 2007; Rodrigues et al., 2010) and with GS 1 as recorded in the Greenland ice cores (Johnsen et al., 2001; Lowe et al., 2008).

3.3.4. Heinrich Stadials

Previous studies on the western Iberian margin have shown that HS are characterized by a synchronous drop of SST and increases in the percentage of the polar species *N. pachyderma* sinistral (e.g., Cayre et al., 1999; de Abreu et al., 2003; Eynaud et al., 2009; Naughton et al., 2009; Salgueiro et al., 2010). We, therefore, mostly delimited the different HS on the basis of the SST records (Fig. 3). HS1 is then recorded between 18 and 15 ka BP, HS2a between 24.5 and 23.2 ka BP; HS2b between 26.1 and 25 ka BP, and HS3 between 30.6 and 29.2 ka BP (Fig. 3). This is in agreement with the age limits previously observed for this region (e.g., de Abreu et al., 2003; Naughton et al., 2009; Salgueiro et al., 2010).

4. Results

4.1. Paleotemperature

In the fifteen cores recovered along the Iberia margin, *G. bulloides* δ^{18}O and SST values vary between 0 and 3.5‰ and 4–24 °C, respectively, over the last 35 ky (Figs. 3 and 4).

The Holocene is marked by the lightest G. *bulloides* δ^{18}O and highest SST averaged values reflecting interglacial warm conditions (Figs. 3 and 4). The spatial distribution of SST over this period clearly shows a latitudinal gradient along the western Iberian margin, varying between 16 and 17 °C in the north and 20–23 °C in the south. The same pattern as in the modern satellite data is detected in the Recent reconstruction, as revealed by mean SST values varying between 16–19 °C and 18–20 °C in the north and 23 °C in the south. Both the Recent and Holocene (8 ky) reconstructions illustrate a tongue of colder SST (by 2–3 °C) close to the coast that extends down to Sines (Fig. 5). Site PO200-10-28-1 is, however, relatively warm compared to the neighboring sites in the Holocene map (site not represented in the Recent reconstruction), but still within the range of the satellite SST. Although the satellite data record SST slightly warmer than the Holocene and Recent reconstructions, this tongue is still reflected in the map. Assuming, that a 12 year long satellite record is in general representative for conditions during the last 1000 years, the transfer function is either underestimating the SST in areas of lower SST or the planktonic foraminifer fauna in these regions is biased towards periods of upwelling. The larger difference between the Holocene Recent and modern satellite conditions was in fact recorded in two sites located close to the coast, MD03-2697 and MD95-2041 (Fig. 5) that are more strongly influenced by cold and highly productive, upwelled waters. On the other hand, small differences are observed in the offshore sites (SU92-03, N3kF24, OMEXII-5K, MD95-2039, D11957P, MD95-2042).

The LGM is marked in every record by relatively stable δ^{18}O *G. bulloides* values, varying from 2‰ in the south (MD99-2339, M39029-7, MD95-2041 and MD95-2042) to 3‰ in the north (MD99-2331 and OMEXII-5K), indicating cooler conditions (Fig. 3). However, the almost absence of *N. pachyderma* (sinistral) and the relatively high SST values (15.5 °C on average) suggest that the LGM was indeed warm. Although warmer, the LGM was slightly colder than the Holocene (<8 ky) (19.1 °C on average; Figs. 4 and 5). The amplitude of SST changes between the LGM and Holocene is, however, complex when comparing site to site, varying between 3 and 10 °C (Fig. 5). Most nearshore records along the western Iberian margin have small LGM − Holocene SST differences (1.5 °C) while very high differences (3–6 °C) are seen further offshore. Clear cold-water conditions are detected around 42°N, in cores OMEXII-9K (11.6 °C) and N3KF24 (11.3 °C).

The YD is marked by heavy *G. bulloides* δ^{18}O (1.5–2‰) values and the presence of polar foraminifera species *N. pachyderma* (sinistral) in most sites (Fig. 3), reflecting cold conditions in the western Iberian Margin. The coldest conditions are recorded in the most offshore records at 39°N, with SST values ranging between 8.6 and 12.5 °C (Figs. 4 and 6). Close to the coast SST varies between 14.1 and 19.1 °C being just lightly colder (1–4 °C) than the Holocene (<8 ky) (Figs. 4–6).

The heaviest *G. bulloides* δ^{18}O values (2–3.5‰) together with the highest *N. pachyderma* (sinistral) percentages (reaching 90% in the northernmost core), and lowest average SST values (from 5 to 11 °C), mark the 3 well-known episodes of iceberg discharges into the North Atlantic, i.e. HS1-3 (Figs. 3, 4 and 6). Every HS is marked by a tongue of cold waters penetrating from north to the south along the Iberian margin, producing a strong SST gradient of about 6 °C (Fig. 6). HS1 and HS3 are the coldest events with SST varying between 5 and 11 °C whereas HS2a and HS2b are less cold (8–11 °C). In general, the cold front extended from the Tore seamount (offshore at 12°W) down into the Gulf of Cadiz. In contrast, the cold front was located just south of Lisbon during H2b. During HS2a, the front was in a position similar to that observed during HS1 and 3, but only reached the latitude of Sines (38°N). The coldest waters, in NNW-SSE direction, are best observed during

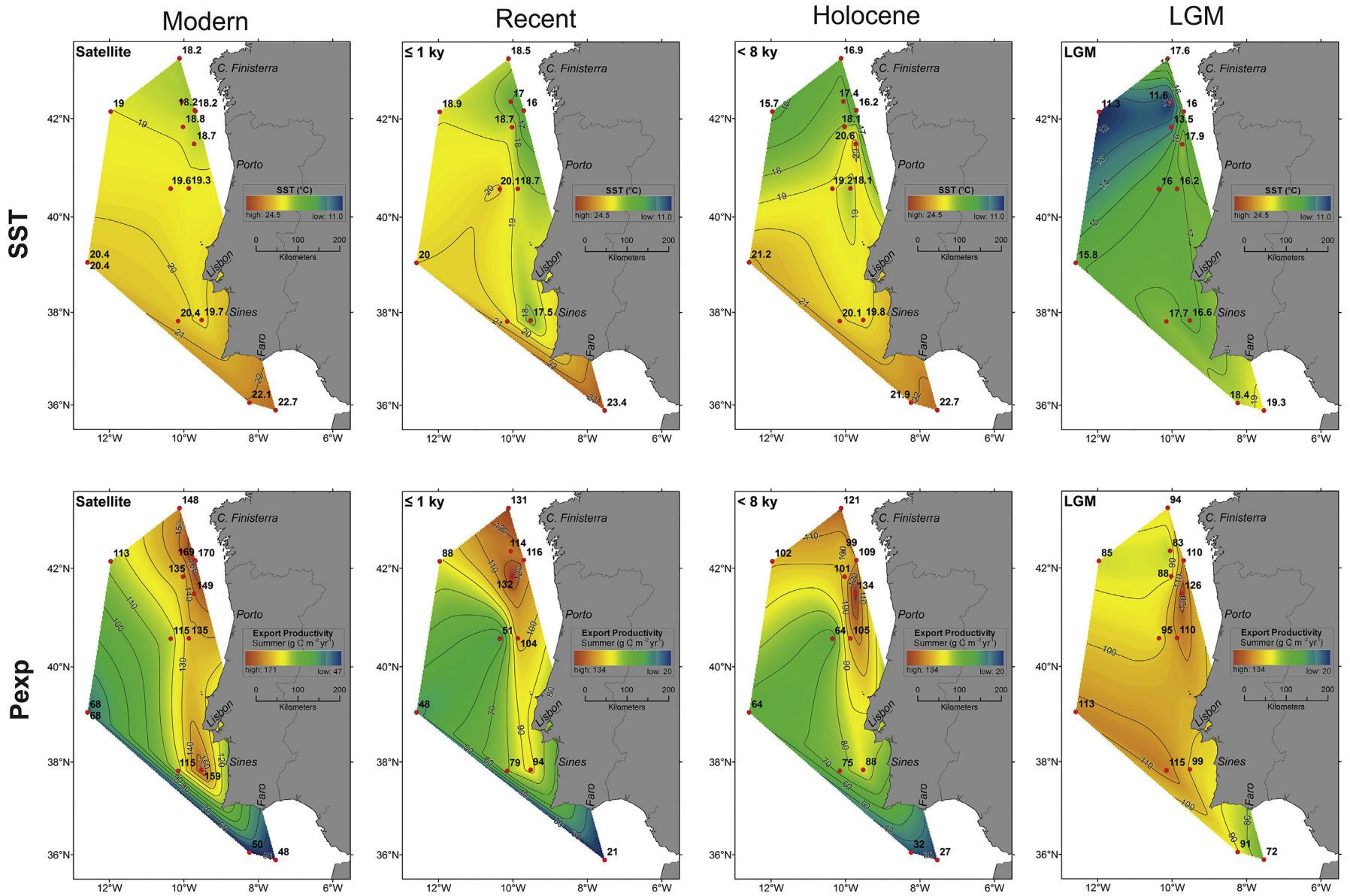

Fig. 5. Summer sea surface temperature (SST) (°C) and export productivity (Pexp) (gC/m2/y) reconstructions based on 15 sediment cores for the time-slices: Modern/Present-day conditions; Holocene (Recent and <8 ky); and Last Glacial Maximum (LGM). The summer sea surface temperature (SST) and export productivity (Pexp) Modern conditions is the interpolation of satellite-derived SST and Pexp (http://www.science.oregonstate.edu/ocean.productivity; Behrenfeld and Falkowski, 1997). Holocene Recent displays the planktonic foraminifera derived SST and Pexp from the uppermost sample for each core record. The other maps show planktonic foraminifera derived SST and Pexp and the average values with standard deviations are available in the supplementary material. Scale for SST ranges from 11 to 24.5 °C and for Pexp from 20 to 134 gC/m^2/y, except for the Modern Pexp map with a range from 47 to 171 gC/m^2/y.

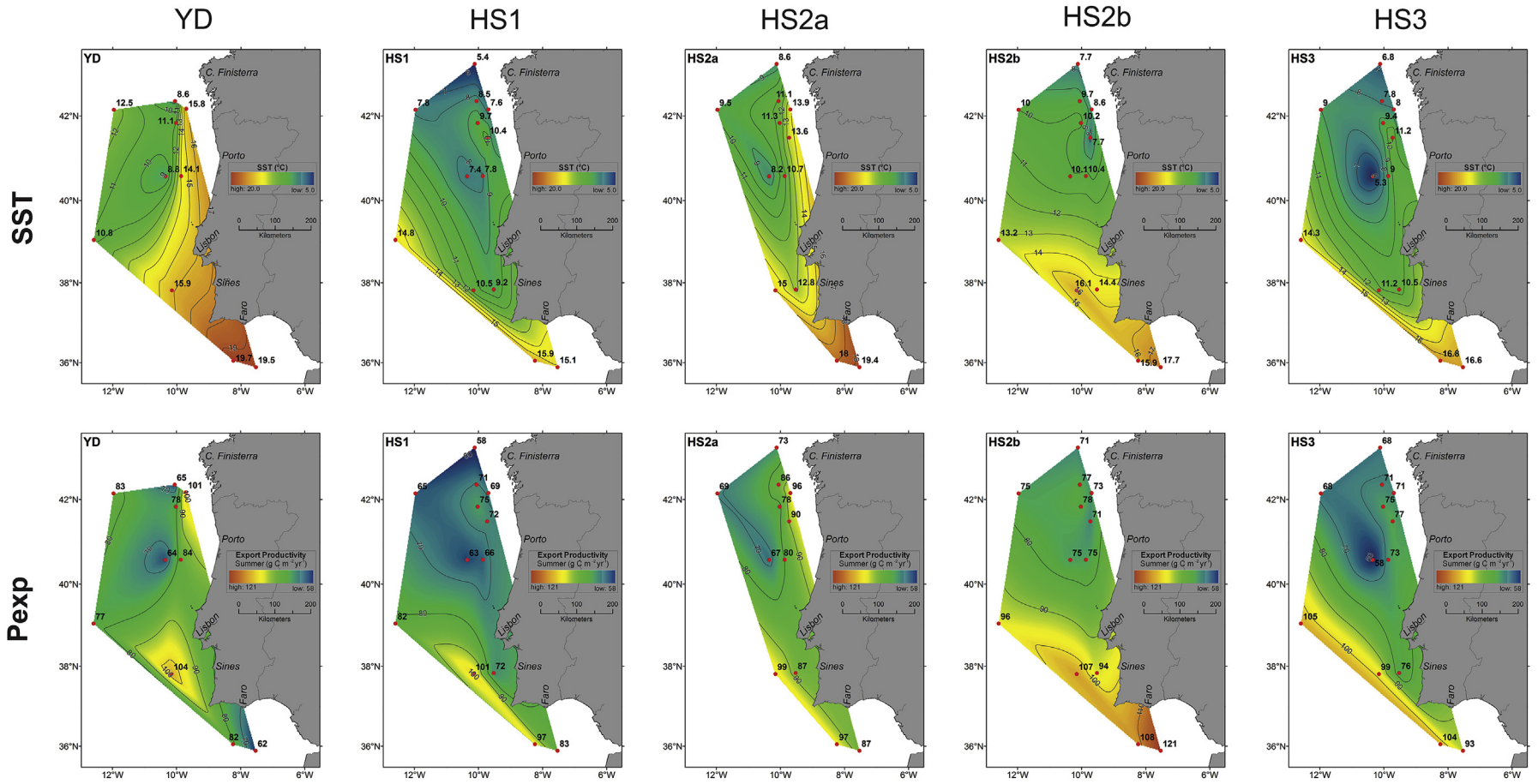

Fig. 6. Summer sea surface temperature (SST) (°C) and export productivity (Pexp) (gC/m^2/y) maps, based on data from 15 sediment cores, for the time slices: Younger Dryas (YD) and Heinrich stadials. The average values with standard deviations are available in the supplementary material.Scale for SST ranges from 5 to 20 °C and for Pexp from 58 to 121 gC/m^2/y.

HS1, 2a, and 3 with the lowest SST values recorded at sites SU92-03 and MD95-2039.

4.2. Paleoproductivity

The modern satellite data map (http://www.science.oregonstate.edu/ocean.productivity/; Behrenfeld and Falkowski, 1997) shows a latitudinal gradient along the western Iberian margin with Pexp varying between 148 gCm^2yr^{-1} in the N and 48 gCm^2yr^{-1} in the south. In the Recent and Holocene (8 ky average) reconstructions Pexp shows the same spatial pattern as SST and latitudinal gradient along the western Iberian margin. During the reconstruction for the Recent Pexp varied between 131 and 21 gCm^2yr^{-1} while in the Holocene Pexp range from 121 gCm^2yr^{-1} to 27 gCm^2yr^{-1} from north to south, respectively.

In both reconstructions and the satellite data, high productivity ($\geq$90 gCm^2yr^{-1}) with maximum Pexp values north of 40°N, coincides with the low SST tongue observed close to the coast down to the Sines latitude. The higher values are defined by cores SU92-03, MD99-2331, OMEXII-5K, OMEXII-9K PO200-10-28-1, MD95-2040, and MD95-2042. On the other hand, low productivity values occur further offshore (west of 10°W) and south of 41°N. The Recent reconstruction, in general, records lower Pexp than the modern satellite data, especially close to the coast. Like the SST reconstructions, the Pexp transfer function seems to underestimate the productivity. This might be the result of the higher resolution grid (9 km) used in the interpolation of the modern satellite than the one applied for reconstruct the Recent conditions. The large difference between the Holocene-Recent and modern data was observed for both SST and Pexp in cores MD03-2697 and MD95-2041, and Pexp in core MD95-2039, which are located close to the coast and under the influence of cold upwelled waters (Fig. 5). In contrast, small differences were found in the offshore sites (SU92-03, N3KF24, OMEXII-5K, D11957P), just as for SST.

Although not reflected in the Holocene averages, Pexp decreased abruptly from 90 to 100 gCm^2yr^{-1} to 40–50 gCm^2yr^{-1} between 8 and 4 ka in the more offshore sites (MD95-2039, MD01-2446 and MD95-2042; Fig. 4), while SST remained constant.

The spatial distribution of Pexp during the LGM (Fig. 5) shows in general higher values (mean 98 gCm^2yr^{-1}) than those recorded over the Holocene (Recent mean: 89 gCm^2yr^{-1}; Holocene mean: 86 gCm^2yr^{-1}), but with the same latitudinal north-south pattern, although the northernmost site (SU92-03) only records 94 gCm^2yr^{-1}. Highest values (110–126 gCm^2yr^{-1}) are detected between 40 and 42°N, at the Tore seamount (D11957P) and offshore Sines (site MD95-2042) with values in the order of 113–115 gCm^2yr^{-1}. The lowest productivity values (between 70 and 95 gCm^2yr^{-1}) are associated with low SST in sites located at 42°N (OMEXII-9K, N3KF24), and in the two sites from the Gulf of Cadiz (M39029-7 and MD99-2339).

During the YD Pexp is lower (mean 80 gCm^2yr^{-1}) than over the LGM, with the lowest Pexp values (62–84 gCm^2yr^{-1}) observed at the Tore seamount and in the Gulf of Cadiz. The highest Pexp (>101 gCm^2yr^{-1}) were recorded off Vigo (MD03-2697, about 42°N) and offshore of Sines (MD95-2042, about 38°N) (Fig. 6).

Coinciding with the tongue of cold surface waters extending down along the western Iberian margin, Pexp was extremely reduced during each HS episode. Actually, in all northwestern records, the Pexp minima during the last 35 ky were detected during the HS (Fig. 4). As observed for the SST, a strong N–S Pexp gradient, between 25 and 35 gCm^2yr^{-1}, is clearly evident (Fig. 6). HS1 and HS3 recorded lower Pexp (58–80 gCm^2yr^{-1}) than HS2a and HS2b (71–80 gCm^2yr^{-1}), and the Pexp boundary, just like SST, extended from the Tore seamount (offshore at 12°W) down into the Gulf of Cadiz, with exception of HS2b, when the front was located south of Lisbon.

Also the lower Pexp is coincident with the coldest waters during HS1, 2a, and 3 but with the lowest Pexp values recorded in sites SU92-03 and MD95-2039.

5. Discussion

The SST and Pexp reconstructions for key time slices (Holocene, LGM, YD, HS) provide insights into the behavior of the upwelling system and major hydrological changes over the last 35 ky (Figs. 3–6).

5.1. Holocene

5.1.1. Recent

The Recent SST distribution pattern, i.e., SST deduced from the uppermost samples in each core, and the map based on the modern SST satellite data show the same patterns (Fig. 5), but with slightly colder Recent SST north of 40° N and off Sines. The major differences were found in the sites located closer to the coast, i.e. sites more likely experiencing colder SST due to upwelling. Some of the temperature difference might be related to the warming of the oceans during the last decades (Levitus et al., 2009). However, underestimation of SST in relation to upwelling was already observed during the transfer function calibration, although the residuals (SST observed − SST estimated) are not significant (Supplementary Fig. 2) on the Portuguese margin (Salgueiro et al., 2010). In fact, the tongue of low, coastal-upwelling related SST that extends down to Sines in the Modern conditions map is easily identified in the reconstructions as well as the N–S temperature gradient. The reconstructed band of cold upwelled waters also fits well with faunal evidence recorded in the surface sediments along the Iberian Margin, that is, increased abundance of the upwelling-related diatom genus *Chaetoceros* and planktonic foraminifera *G. bulloides* (Abrantes, 1988; Salgueiro et al., 2008). Such features are the mark of the hydrology and of regional coastal upwelling variability, with stronger and more persistent upwelling north of 40°N extending well offshore (Haynes et al., 1993). Lower SST occurs also between Lisbon and Sines, possibly reflecting the presence of the important Cape da Roca filament. Warmer waters are depicted west of 10°W and south of 41°N and also in a very coastal region along the SW coast and north of Lisbon, exactly as in the Modern conditions, reflecting the presence of the Iberian Poleward Current (Peliz et al., 2005).

As coastal upwelling brings colder waters rich in new nutrients into the system (Dugdale and Goering, 1967), primary productivity in these regions is the highest of all the oceanic provinces and a significant proportion consists of new production (Hill et al., 1998) and consequently Pexp (portion of the net primary production that is exported to the bottom ocean). For this reason, the Modern high Pexp conditions coincide with the low SST. In the Recent record, the presence of both a high Pexp tongue and its N–S gradient, confirm that the high productivity generated by the nutrient input of the cold subsurface waters upwelled near the coast is sustained. Furthermore, the association between warmer, subtropical waters and lower Pexp values observed for the Modern conditions is also maintained. The larger decrease in Pexp is observed for the upwelling-influenced sites. One has to keep in mind, however, that the satellite data used in the calibration (Salgueiro et al., 2010), and the current reconstructions, has a lower spatial resolution than the one plotted in the Modern conditions. Nevertheless, the patterns should remain the same, because both data sets are correlated (Supplementary Figs. 2 and 3), and only the absolute values will differ.

5.1.2. Last 8 ky

In the studied records, the Holocene is marked by lower *G. bulloides* $\delta^{18}O$ (Fig. 2) and high SST values (Fig. 4) reflecting warm

interglacial conditions, in agreement with previous studies (e.g., de Abreu et al., 2003; Rodrigues et al., 2010; Salgueiro et al., 2010). The spatial SST distribution along the western Iberian margin clearly shows SST increases from north to south and east to west. The cold waters in the north and close to the coast reflect the prevailing influence of the colder Paleo-Portugal Current and Paleo-Portugal Coastal Current in the north, and of the subtropical Paleo-Azores Current in the south and offshore (Fig. 5). As discussed for the Recent, colder SSTs closer to the coast clearly demonstrate the influence of coastal upwelling centers. In general, the pattern in the Holocene and Recent map follows the one observed for modern conditions, emphasizing the quality of the planktonic foraminifera reconstructions (Salgueiro et al., 2010). The lowest SST values are coincident with highest Pexp, except for site PO200-10-28-1, and located in the north off Galicia and along of the coast until Sines. All sites in the north are likely to be recording the lasting presence of the filaments, with consistently high productivity (Fig. 4). Similarly, core MD95-2041 on the Sines coast is recording the southward extension of the Cabo da Roca (close to Lisbon) upwelling filament. The lowest Pexp values are observed in the oligotrophic waters offshore and in the Gulf of Cadiz (Fig. 5). Such distribution resembles the present-day oceanography linked to the Iberian Poleward and Azores Currents and thus indicate that in general the actual conditions have been maintained throughout the Holocene.

One peculiar feature of Holocene climate variability in the three offshore sites MD95-2039, MD01-2446 and MD95-2042 (Fig. 4) is the strong Pexp decrease between 8 and 4 ka, at times of constant SST. The same feature has been observed in the coccolith productivity record of core MD03-2699 at 39°N 10.4°W (Palumbo et al., 2013), confirming the occurrence of less productive conditions as a whole. Such conditions may be due to a decrease in nutrient availability mainly in the northernmost offshore waters, which might be related to a decrease in nutrient levels of the Paleo-Portugal Current waters. To disentangle the causes of this occurrence further work is needed.

5.2. Last Glacial Maximum

Atlantic Ocean-basin wide SST reconstructions for the LGM show a strong cooling in latitudes north of 40°N (Pflaumann et al., 2003; Kucera et al., 2005) that led to a 30–40% reduction in the Atlantic Meridional Overturning Circulation (McManus et al., 2004) Cooling was stronger in the western than in the eastern Atlantic basin, and, for the three sites on the Iberian margin, reconstructed SST differences between modern and LGM are in the range of 2 °C (Kucera et al., 2005; MARGO project members, 2009) to 4 °C (Pflaumann et al., 2003). Previous studies already showed that SST remained relative warm on the Iberian margin (Abrantes, 1988; de Abreu et al., 2003; Voelker et al., 2009; Salgueiro et al., 2010; Penaud et al., 2011; Voelker and de Abreu, 2011). Our data confirms the presence of warm conditions during the LGM, although relatively colder than those characterizing the Holocene and present-day (Figs. 2, 4 and 5). The spatial LGM SST distribution is, however, more complex: 1) the inshore sites record small amplitude differences between the LGM and Holocene, whereas 2) the offshore sites experienced larger differences. Furthermore, 3) there is a clear cold-water tongue around 42°N (Fig. 5). The cold-water tongue could represent an eastward extension of the much colder SST observed in the open North Atlantic by Kucera et al. (2005) and Pflaumann et al. (2003). The lower inshore SST gradient may reflect a stronger and more coastal influence of subtropical waters from the Paleo-Iberian Poleward Current. Indeed, Voelker et al. (2009) and Salgueiro et al. (2010) observed that during the LGM the winter circulation off the western Iberian margin was similar to that of present-day. The relative higher SST accompanied by the presence of the subtropical planktonic foraminifera *Globigerinoides ruber* (white), as previously shown by Salgueiro et al. (2010), is another indication that Paleo-Iberian Poleward Current waters reached the northernmost site SU92-03. The high thermal gradient observed between the North and the South, on the other hand, can be explained by the southward displacement of the Polar Front and associated stronger advection of subpolar waters by the Paleo-Portugal Current.

Pexp is in general higher during the LGM than during the Holocene and present-day. The high values between 40 and 42°N, offshore of Sines and at the Tore seamount seems to result from the strengthening of northerly alongshore winds and the sea-level minimum, favoring the intensification and displacement of the coastal upwelling centers further west. Indeed, climate simulations have shown the prevalence of either northerly alongshore winds on the Iberian margin (at least in winter; Hosletler et al., 1999) and strengthened trade winds in NW Africa (Broccoli et al., 2006). High dust content, leading to the strengthening of the trade winds, was detected during the LGM in the northwestern Africa (Jullien et al., 2007). Also, the high Pexp in western Iberian margin is also supported by previous works on the area (Abrantes, 2000), which shows an increase of diatom fluxes in the area during the LGM. The highest Pexp was recorded in the cores close to the coast, supporting the existence of an upwelling situation similar to the present-day. The slightly reduced value of Pexp in core SU92-03 might indicate a reduction of the upwelling off Cape Finisterra rather than an enhancement as in all the other upwelling cells along the margin. The high Pexp at Tore seamount is in the range of the one observed in the upwelling cells to its north and south, which strengthens the idea that the upwelling front might have been extended to this offshore location (Lebreiro et al., 1997). The lowest productivity is detected in the cold-water tongue around 42°N pointing to a causal link between both.

In the Gulf of Cadiz, the observed warm SST and high Pexp (Fig. 5) indicate that this region has been continually influenced by the subtropical Paleo-Azores Current, in agreement with the proposed extension of the Azores Front into the Gulf of Cadiz (Rogerson et al., 2004). Nevertheless, Pexp values are higher than during the Holocene, suggesting that productive conditions have also occurred in the region either due to frontal upwelling or as a reflection of the closer position to the Portuguese coastal upwelling filaments that, caused by the lower sea-level, extended further offshore than today.

5.3. Younger Dryas

In the North Atlantic, the YD (GS1) is generally marked by surface-water cooling linked to an almost full return to glacial conditions and a reduction in the Atlantic Meridional Overturning Circulation (Labeyrie and Party, 1992; McManus et al., 2004; Brauer et al., 2008). Records off NW Africa also recorded high upwelling-related productivity (e.g., Romero et al., 2008; Penaud et al., 2010, 2011). In the Iberian margin, the YD is well recorded off Lisbon with cold temperatures (8 °C; Rodrigues et al., 2010) but less severe, although identifiable, in other records (Figs. 2 and 4), in agreement with previous observations (e.g., Abrantes et al., 1998; Bard et al., 2000; Hall and McCave, 2000; Schönfeld and Zahn, 2000; Turon et al., 2003). The cooling is, however, less than expected in comparison to other GS and not obvious in all records. The time slice map sheds some light into the problem because it clearly shows an influx of warmer Paleo-Azores Current waters (14–19 °C) into the southern margin and then extending to the northern slope (Fig. 6). As a result, at the sites influenced by the warmer waters, SST only dropped by about 2 °C. This water mass may also have pushed colder waters offshore, where the real impact of the YD cooling

would then have been felt, mainly north of 39°N, by large amplitude changes.

In the offshore region, Pexp was relatively low, as expected for nutrient-poor subtropical waters. However, there are two regions with relatively high Pexp: at the northernmost west coast, off Vigo (about 42°N), and offshore of Sines (about 38°N). The NW Iberian region coincides with the present-day position of the stronger and more persistent coastal upwelling center (Haynes et al., 1993; Fiúza et al., 1998) that is also fed by nutrients supplied by river runoff (Abrantes and Moita, 1999). River supply of nutrients is likely to have been high during the YD, as observed for the Tagus River (Rodrigues et al., 2010). Offshore Sines, Pexp shows the second highest values (after LGM) consistent with biomarker and organic carbon data (Pailler and Bard, 2002). Given the SST evidence for a strong influence of subtropical waters along the inner coast, such as under modern conditions, we suspect that the increased productivity might be a mark of the productivity associated to the Cape da Roca filament (not clearly defined due to a lack of spatial resolution, but clearly seen in the modern data).

5.4. Heinrich Stadials

During HS the Polar Front was pushed south to the latitudes of the Iberian margin thereby greatly impacting climate in this region (e.g., Bard et al., 2000; Pailler and Bard, 2002; de Abreu et al., 2003; Voelker et al., 2006; Naughton et al., 2009; Salgueiro et al., 2010). Although HS2a, 2b and 3 with durations of 1.3 ky, 1.1 ky and 1.4 ky, respectively, lasted only half as long as HS1, similar features are seen in the SST and Pexp maps of all four events (Fig. 6). A tongue of cold, subpolar waters extended along the margin producing a strong SST gradient of about 10 °C (Fig. 6) that is believed to reflect the path of the Paleo-Portugal Current. Indeed, the southward penetration of iceberg-laden meltwaters generated a substantial drop not only in SST but also in Pexp (Figs. 4 and 6). Another identical feature is the establishment of a front off the southern margin separating the subpolar waters in the north from the transitional to subtropical ones in the south. During HS1 and HS3 the front extended from the Tore seamount (offshore at 12°W) down into the Gulf of Cadiz. However, a latitudinal front was located just south of Lisbon during HS2b. Through HS2a, the front was in a position similar to the one observed in HS1 and 3, but warm waters also stretched northward as a slope current, most likely a Paleo-Iberian Poleward Current (Fig. 6) and an extension into this region of a paleo-version of the Azores Front during the Last Glacial (Rogerson et al., 2004; Voelker and de Abreu, 2011). The warm waters and related front (Paleo-Azores Front) at the southern margin clearly contradict the climate model results of meltwater hosing experiments that due to a strong eastern boundary current (Portugal Current combined with Canary Current) have the tongue of cold surface waters extending further south than the Canary Islands (e.g., Prange et al., 2004; Kageyama et al., 2010; Mariotti et al., 2012).

Although Pexp was reduced in the subpolar waters, the mean values were still in the range of those observed in the offshore region during the Holocene (Figs. 5 and 6). In these waters productivity was likely related to spring and fall blooms as in the modern subpolar regime (Levy et al., 2005). During HS2a, Pexp was slightly higher in the coastal band under warmer water influence, maybe indicating that the subtropical surface and subsurface waters were nutrient-richer than their subpolar counterparts during the HS (in reverse to the modern situation). Nutrient refurbishment in the subpolar waters is likely to have been hampered by the sea ice cover and shallower mixed layer depth (Mariotti et al., 2012). During all HS, Pexp was high near and south of the observed front (Fig. 6) indicating that frontal upwelling, as typical along the Azores Front today (Fasham et al., 1985), most likely caused this increase in productivity.

6. Conclusions

Time slice mapping of SST and Pexp based on fifteen cores distributed along the Iberia margin reveals patterns of SST and productivity during periods marked by climatic and oceanographic re-organizations, such as: Holocene (Recent and last 8 ky), the LGM, YD, and HS.

SST and Pexp in the Holocene (Recent and 8 ky) show the presence of low SST/high Pexp waters all along the western Portuguese margin, as well as a latitudinal SST gradient of 6 °C from north to south. This pattern can easily be explained as a record of a coastal upwelling system similar to the modern one.

The LGM was only slightly colder than the Holocene and present-day (mean: 15.5 °C), but a complex spatial SST distribution suggests a circulation pattern of the western Iberian margin similar to their modern counterpart, with an offshore southward flow of subpolar waters by a Paleo-Portugal Current and an inshore poleward inflow of subtropical waters, a Paleo-Iberian Poleward Current. In terms of productivity, the LGM was the most productive of all the investigated periods, with a Pexp spatial distribution that is likely to reflect a westward displacement of the coastal upwelling centers lead to the strengthening of winds and sea-level minima.

During the YD a longitudinal thermal front is located at 10°W with colder transitional waters offshore and warmer subtropical waters inshore, suggesting a stronger northward influence of the subtropical current (Paleo-Iberian Poleward Current) that also forces the colder waters offshore.

During the HS events, the southward penetration of icebergs-derived meltwater generated a substantial cooling and a drop in productivity. HS1 was the coldest followed by HS3 and HS2. Besides the extreme cold conditions, a strong N–S SST gradient of about 6 °C also marks the Iberian margin during these episodes. Productivity was generally very low, but slightly higher near and south of the SST subtropical front, which is separating the colder waters in the north from the subtropical ones in the south. The higher productivity in the south is possibly linked to nutrient advection along an Azores-like Frontal system.

Acknowledgments

This study was funded by the Portuguese Foundation for Science and Technology (FCT) fellowships SFRH/BPD/26525/2006 and SFRH/BPD/36615/2007 to E. Salgueiro, and F. Naughton, respectively. The authors also wish to thank R. O'Malley and M. Behrenfeld for the summer satellite average data used in Modern Conditions images. ES and AV also acknowledge funding support from EU COST Action ES0907 "INTIMATE: INTegrating Ice core, MArine and TErrestrial records (60 000 to 8000 years ago)".

Appendix A. Supplementary data

Supplementary data related to this article can be found at http://dx.doi.org/10.1016/j.quascirev.2014.09.001.

References

Abrantes, F., 1988. Diatom productivity peak and increased circulation during Latest Quaternary – Alboran Basin (Western Mediterranean). Mar. Micropaleontol. 13, 79–96.

Abrantes, F., 1991. Increased upwelling off Portugal during the last glaciation: diatom evidence. Mar. Micropaleontol. 17, 285–310.

Abrantes, F., 1992. Paleoproductivity oscillations during the last 130 ka along the Portuguese and NW African margins. In: Summerhayes, C.P., Prell, W.L.,

Emeis, K.C. (Eds.), Upwelling Systems: Evolution since the Early Miocene. The Geological Society, London, pp. 499–510.
Abrantes, F., 2000. 200 000 yr diatom records from Atlantic upwelling sites reveal maximum productivity during LGM and a shift in phytoplankton community structure at 185 000 yr. Earth Planet. Sci. Lett. 176, 7–16.
Abrantes, F., Baas, J., Haflidason, H., Rasmussen, T., Klitgaard, D., Loncaric, N., Gaspar, L., 1998. Sediment fluxes along the northeastern European Margin: inferring hydrological changes between 20 and 8 kyr. Mar. Geol. 152, 7–23.
Abrantes, F., Moita, M.T., 1999. Water column and recent sediment data on diatoms and coccolithophorids, off Portugal, confirm sediment record of upwelling events. Oceanol. Acta 22, 319–336.
Alberto, A.I.M., 2012. Variações da temperatura de superfície e produtividade oceânicas ao largo da margem ibérica durante os últimos 20 000 anos. Faculdade de Ciências e Tecnologia. Universidade do Algarve.
Alvarez-Salgado, X.A., Figueiras, F.G., Perez, F.F., Groom, S., Nogueira, E., Borges, A., Chou, L., Castro, C.G., Moncoiffe, G., Rios, A.F., Miller, A.E.J., Frankignoulle, M., Savidge, G., Wollast, R., 2003. The Portugal coastal counter current off NW Spain: new insights on its biogeochemical variability. Prog. Oceanogr. 56, 281–321.
Antoine, D., André, J.-M., Morel, A., 1996. Oceanic primary production: 2. Estimation at global scale from satellite (Coastal Zone Color Scanner) chlorophyll. Glob. Biogeochem. Cycles 10, 57–69.
Bard, E., Rostek, F., Menot-Combes, G., 2004. Radiocarbon calibration beyond 20,000 C-14 yr BP by means of planktonic foraminifera of the Iberian Margin. Quat. Res. 61, 204–214.
Bard, E., Rostek, F., Turon, J.-L., Gendreau, S., 2000. Hydrological impact of heinrich events in the subtropical Northeast Atlantic. Science 289, 1321–1324.
Behrenfeld, M.J., Falkowski, P.G., 1997. Photosynthetic rates derived from satellite-based chlorophyll concentration. Limnol. Oceanogr. 42, 1–20.
Brauer, A., Haug, G.H., Dulski, P., Sigman, D.M., Negendank, J.F.W., 2008. An abrupt wind shift in western Europe at the onset of the Younger Dryas cold period. Nat. Geosci. 1, 520–523.
Broccoli, A.J., Dahl, K.A., Stouffer, R.J., 2006. Response of the ITCZ to Northern Hemisphere cooling. Geophys. Res. Lett. 33 http://dx.doi.org/10.1029/2005GL024546.
Cayre, O., Lancelot, Y., Vincent, E., Hall, M.A., 1999. Paleoceanographic reconstructions from planktonic foraminifera off the Iberian margin: temperature, salinity, and Heinrich events. Paleoceanography 14, 384–396.
Chabaud et al., submitted to The Holocene. Land-sea climatic variability in the eastern North Atlantic subtropical region over the last 14,200 years: atmospheric and oceanic processes at different timescales.
Colmenero-Hidalgo, E., Flores, J.-A., Sierro, F.J., Bárcena, M.Á., Löwemark, L., Schönfeld, J., Grimalt, J.O., 2004. Ocean surface water response to short-term climate changes revealed by coccolithophores from the Gulf of Cadiz (NE Atlantic) and Alboran Sea (W Mediterranean). Palaeogeogr. Palaeoclimatol. Palaeoecol. 205, 317–336.
de Abreu, L., 2000. High Resolution Palaeoceanography off Portugal during the Last Glacial Cycles. University of Cambridge, Cambridge, p. 366.
de Abreu, L., Shackleton, N.J., Schoenfeld, J., Hall, M., Chapman, M., 2003. Millennial-scale oceanic climate variability off the Western Iberian margin during the last two glacial periods. Mar. Geol. 196, 1–20.
de Abreu, L., 1995. Biostratigrafia e paleoecologia dos foraminíferos planctónicos Quaternários da Montanha submarina da Galicia (Margem Oeste-Ibérica) (Master thesis). University of Lisbon, p. 173.
Dugdale, R., Goering, J., 1967. Uptake of new and regenerated forms of nitrogen in primary productivity. Limnol. Oceanogr. 12, 196–206.
Eberwein, A., Mackensen, A., 2008. Last Glacial Maximum paleoproductivity and water masses off NW-Africa: evidence from benthic foraminifera and stable isotopes. Mar. Micropaleontol. 67, 87–103.
Elliot, M., Labeyrie, L., Bond, G., Cortijo, E., Turon, J.L., Tisnerat, N., Duplessy, J.C., 1998. Millennial-scale iceberg discharges in the Irminger Basin during the Last Glacial period: relationship with the Heinrich events and environmental settings. Paleoceanography 13, 433–446.
Eppley, R.W., Peterson, B.J., 1979. Particulate organic-matter flux and planktonic new production in the deep ocean. Nature 282, 677–680.
Eynaud, F., de Abreu, L., Voelker, A., Schönfeld, J., Salgueiro, E., Turon, J.-L., Penaud, A., Toucanne, S., Naughton, F., Sanchez Goni, M.F., Malaize, B., Cacho, I., 2009. Position of the polar front along the western Iberian margin during key cold episodes of the last 45 ka. Geochem. Geophys. Geosyst. 10, Q07U05. http://dx.doi.org/10.1029/2009GC002398.
Fasham, M.J.R., Platt, T., Irwin, B., Jones, K., 1985. Factors affecting the spatial pattern of the deep chrolophyll maximum in the region of the Azores Front. In: Crease, J., Gould, W.J., Saunders, P.M. (Eds.), Essays on Oceanography: a Tribute to John Swallow. Pergamon, Oxford, pp. 129–166.
Fiúza, A.F.D., Demacedo, M.E., Guerreiro, M.R., 1982. Climatological space and time variation of the portuguese coastal upwelling. Oceanol. Acta 5, 31–40.
Fiúza, A.F.G., 1983. Upwelling patterns off Portugal. In: Suess, E., Thiede, J. (Eds.), Coastal Upwelling its Sediment Record. Plenum Press, New York, pp. 85–98.
Fiúza, A.F.G., 1984. Hidrologia e Dinamica das Aguas Costeiras de Portugal. Faculdade de Ciências da Universidade de Lisboa, Lisbon, p. 294.
Fiúza, A.F.G., Hamann, M., Ambar, I., Diaz del Rio, G., Gonzalez, N., Cabanas, J.M., 1998. Water masses and their circulation off western Iberia during may 1993. Deep Sea Res. Part I: Oceanogr. Res. Pap. 45, 1127–1160.
Frouin, R., Fiuza, A.F.G., Ambar, I., Boyd, T.J., 1990. Observations of a poleward surface current off the coasts of Portugal and Spain during Winter. J. Geophys. Res-Oceans 95, 679–691.
Hall, I.R., McCave, I.N., 2000. Palaeocurrent reconstruction, sediment and thorium focussing on the Iberian Margin over the last 140 ka. Earth Planet. Sci. Lett. 178, 151–164.
Haynes, R., Barton, E., Pilling, I., 1993. Development, persistence, and variability of upwelling filaments off the Atlantic coast of the Iberian Peninsula. J. Geophys. Res. 98, 22681–22692.
Hill, E.A., Hickey, B.M., Shillington, F.A., Strub, P.T., Brink, K.H., Barton, E.D., Thomas, A.C., 1998. Eastern ocean boundaries coastal segment. In: Robinson, A.R., Brink, K.H. (Eds.), The Sea. John Wiley and Sons, New York, pp. 29–67.
Hosletler, S.W., Clark, P.U., Bartlein, P.J., Mix, A.C., Pisias, N.J., 1999. Atmospheric transmission of North Atlantic heinrich events. J. Geophys. Res. 104, 3947–3952.
Imbrie, J., Hays, J.D., Martinson, D.G., Mcintyre, A., Mix, A.C., Morley, J.J., Pisias, N.G., Prell, W.L., Shackleton, N.J., 1984. The orbital theory of Pleistocene climate: support from a revised chronology of the marine N18O record. In: al, B.e. (Ed.), Milankovitch and Climate, Part I. Reidel, Dordrecht, pp. 269–305.
Johnsen, S.J., DahlJensen, D., Gundestrup, N., Steffensen, J.P., Clausen, H.B., Miller, H., Masson-Delmotte, V., Sveinbjornsdottir, A.E., White, J., 2001. Oxygen isotope and palaeotemperature records from six Greenland ice-core stations: camp century, Dye-3, GRIP, GISP2, Renland and NorthGRIP. J. Quat. Sci. 16, 299–307.
Jullien, E., Grousset, F., Malaizé, B., Duprat, J., Sanchez-Goni, M.F., Eynaud, F., Charlier, K., Schneider, R., Bory, A., Bout, V., Flores, J.A., 2007. Low-latitude "dusty events" vs. high-latitude "icy Heinrich events". Quat. Res. 68, 379–386.
Kageyama, M., Paul, A., Roche, D.M., Van Meerbeeck, C.J., 2010. Modelling glacial climatic millennial-scale variability related to changes in the Atlantic meridional overturning circulation: a review. Quat. Sci. Rev. 29, 2931–2956.
Kohfeld, K.E., Quere, C.L., Harrison, S.P., Anderson, R.F., 2005. Role of marine biology in glacial-interglacial CO2 cycles. Science 308, 74–78.
Kucera, M., Rosell-Mele, A., Schneider, R., Waelbroeck, C., Weinelt, M., 2005. Multiproxy approach for the reconstruction of the glacial ocean surface (MARGO). Quat. Sci. Rev. 24, 813–819.
Labeyrie, L., Party, S.S., 1992. Rapport Preliminaire de PALEOCINAT II (Paleocirculation de l'Atlantique nord). IFREMER, INSU.
Lambeck, K., Esat, T.M., Potter, E.K., 2002. Links between climate and sea levels for the past three million years. Nature 419, 199–206.
Lebreiro, S.M., Moreno, J.C., Abrantes, F.F., Pflaumann, U., 1997. Productivity and paleoceanographic implications on the Tore Seamount (Iberian Margin) during the last 225 kyr: foraminiferal evidence. Paleoceanography 12, 718–727.
Levitus, S., Antonov, J.I., Boyer, T.P., Locarnini, R.A., Garcia, H.E., Mishonov, A.V., 2009. Global ocean heat content 1955–2008 in light of recently revealed instrumentation problems. Geophys. Res. Lett. 36 http://dx.doi.org/10.1029/2008gl037155.
Levy, R.C., Remer, L.A., Martins, J.V., Kaufman, Y.J., Plana-Fattori, A., Redemann, J., Wenny, B., 2005. Evaluation of the MODIS aerosol retrievals over ocean and land during CLAMS. J. Atmos. Sci. 62, 974–992.
Loewemark, L., 2001. Biogenic Traces as Paleoceanographic Indicators in Late Quaternary Sediments from the SW Iberian Margin. In: Ber.-Rep., Inst. fur Geowiss, vol. 14. Universitat Kiel, Kiel.
Lowe, J.J., Rasmussen, S.O., Bjorck, S., Hoek, W.Z., Steffensen, J.P., Walker, M.J.C., Yu, Z.C., Grp, I., 2008. Synchronisation of palaeoenvironmental events in the North Atlantic region during the Last Termination: a revised protocol recommended by the INTIMATE group. Quat. Sci. Rev. 27, 6–17.
MARGO project members, 2009. Constraints on the magnitude and patterns of ocean cooling at the Last Glacial Maximum. Nat. Geosci. 2, 127–132.
Mariotti, V., Bopp, L., Tagliabue, A., Kageyama, M., Swingedouw, D., 2012. Marine productivity response to Heinrich events: a model-data comparison. Clim. Past. 8, 1581–1598.
Martinson, D.G., Pisias, N.G., Hays, J.D., Imbrie, J., Moore, T., Shackleton, N.J., 1987. Age dating and orbital theory of the ice ages: development of a high-resolution 0 to 300,00-Year chronostratigraphy. Quat. Res. 27, 1–29.
Martrat, B., Grimalt, J.O., Shackleton, N.J., de Abreu, L., Hutterli, M.A., Stocker, T.F., 2007. Four climate cycles of recurring deep and surface water destabilizations on the iberian margin. Science 317, 502–507.
McManus, J.F., Francois, R., Gherardi, J.M., Keigwin, L.D., Brown-Leger, S., 2004. Collapse and rapid resumption of Atlantic meridional circulation linked to deglacial climate changes. Nature 428, 834–837.
Mix, A.C., Bard, E., Schneider, R., 2001. Environmental processes of the ice age: land, oceans, glaciers (EPILOG). Quat. Sci. Rev. 20, 627–657.
Naughton, F., Goni, M.F.S., Desprat, S., Turon, J.L., Duprat, J., Malaize, B., Joli, C., Cortijo, E., Drago, T., Freitas, M.C., 2007. Present-day and past (last 25 000 years) marine pollen signal off western Iberia. Mar. Micropaleontol. 62, 91–114.
Naughton, F., Sanchez Goñi, M.F., Kageyama, M., Bard, E., Duprat, J., Cortijo, E., Desprat, S., Malaize, B., Joly, C., Rostek, F., Turon, J.L., 2009. Wet to dry climatic trend in north-western Iberia within Heinrich events. Earth Planet. Sci. Lett. 284, 329–342.
Pailler, D., Bard, E., 2002. High frequency palaeoceanographic changes during the past 140 000 yr recorded by the organic matter in sediments of the Iberian Margin. Palaeogeogr. Palaeoclimatol. Palaeoecol. 2799, 1–22.
Palumbo, E., Flores, J.A., Perugia, C., Emanuele, D., Petrillo, Z., Rodrigues, T., Voelker, A.H.L., Amore, F.O., 2013. Abrupt variability of the last 24 ka BP recorded by coccolithophore assemblages off the Iberian Margin (core MD03-2699). J. Quat. Sci. 28, 320–328.
Peliz, A., Dubert, J., Santos, A.M.P., Oliveira, P.B., Le Cann, B., 2005. Winter upper ocean circulation in the Western Iberian Basin – Fronts, Eddies and Poleward Flows: an overview. Deep-Sea Res. Pt I 52, 621–646.

Penaud, A., Eynaud, F., Turon, J.L., Blamart, D., Rossignol, L., Marret, F., Lopez-Martinez, C., Grimalt, J.O., Malaize, B., Charlier, K., 2010. Contrasting paleoceanographic conditions off Morocco during Heinrich events (1 and 2) and the Last Glacial Maximum. Quat. Sci. Rev. 29, 1923–1939.

Penaud, A., Eynaud, F., Voelker, A., Kageyama, M., Marret, F., Turon, J.L., Blamart, D., Mulder, T., Rossignol, L., 2011. Assessment of sea surface temperature changes in the Gulf of Cadiz during the last 30 ka: implications for glacial changes in the regional hydrography. Biogeosciences 8, 2295–2316.

Perez, F.F., Castro, C.G., Alvarez-Salgado, X.A., Rios, A.F., 2001. Coupling between the Iberian basin – scale circulation and the Portugal boundary current system: a chemical study. Deep-Sea Res. Pt I 48, 1519–1533.

Pflaumann, U., Sarnthein, M., Chapman, M., d'Abreu, L., Funnell, B., Huels, M., Kiefer, T., Maslin, M., Schulz, H., Swallow, J., van Kreveld, S., Vautravers, M., Vogelsang, E., Weinelt, M., 2003. Glacial North Atlantic: sea-surface conditions reconstructed by GLAMAP 2000. Paleoceanography 18, 1065. http://dx.doi.org/10.1029/2002PA000774.

Prange, M., Lohmann, G., Romanova, V., Butzin, M., 2004. Modelling tempo-spatial signatures of Heinrich Events: influence of the climatic background state. Quat. Sci. Rev. 23, 521–527.

Reguera, M.I.G., 2001. Paleoceanografıa y estratigrafıa de alta resolucio en el Golfo de Cadiz en los ultimos 40.000 anos mediante el estudio de foraminıferos planctonicos. Departamento de Geologia. Universidad de Salamanca, p. 188.

Relvas, P., Barton, E.D., 2002. Mesoscale patterns in the Cape São Vicente (Iberian Peninsula) upwelling region. J. Geophys. Res. 107, 28-21–28-23.

Rios, A.F., Perez, F.F., Fraga, F., 1992. Water masses in the upper and Middle North-Atlantic ocean east of the azores. Deep-Sea Res. 39, 645–658.

Rodrigues, T., Grimalt, J.O., Abrantes, F., Naughton, F., Flores, J.A., 2010. The last glacial-interglacial transition (LGIT) in the western mid-latitudes of the North Atlantic: abrupt sea surface temperature change and sea level implications. Quat. Sci. Rev. 29, 1853–1862.

Rogerson, M., Rohling, E.J., Weaver, P.P.E., Murray, J.W., 2004. The azores front since the last glacial maximum. Earth Planet. Sci. Lett. 222, 779–789.

Romero, O.E., Kim, J., Donner, B., 2008. Submillennial-to-millennial variability of diatom production off Mauritania, NW Africa, during the last glacial cycle. Paleoceanography 23, PA3218. http://dx.doi.org/10.1029/2008PA001601.

Salgueiro, E., Voelker, A., Abrantes, F., Meggers, H., Pflaumann, U., Loncaric, N., González-Álvarez, R., Oliveira, P., Bartels-Jonsdottir, H., Moreno, J., Wefer, G., 2008. Planktonic foraminifera from modern sediments reflect upwelling patterns off Iberia: Insights from a regional Transfer function. Mar. Micropaleontol. 66, 135–164.

Salgueiro, E., Voelker, A.H.L., de Abreu, L., Abrantes, F., Meggers, H., Wefer, G., 2010. Temperature and productivity changes off the western Iberian margin during the last 150 ky. Quat. Sci. Rev. 29, 680–695.

Sanchez-Goni, M.F., Landais, A., Fletcher, W.J., Naughton, F., Desprat, S., Duprat, J., 2008. Contrasting impacts of Dansgaars-Oeschger events over a western European latitudinal transect modulated by orbital parameters. Quat. Sci. Rev. 27, 1789.

Sarnthein, M., Winn, K., 1988. Global variations of surface ocean productivity in Low and Mid latitudes: Influence on CO_2 reservoirs of the deep ocean and atmosphere during the last 21,000 years. Paleoceanography 3, 361–399.

Schmittner, A., 2005. Decline of the marine ecosystem caused by a reduction in the Atlantic overturning circulation. Nature 434, 628.

Schönfeld, J., Zahn, R., 2000. Late Glacial to Holocene history of the Mediterranean Outflow. Evidence from benthic foraminiferal assemblages and stable isotopes at the Portuguese margin. Palaeogeogr. Palaeocl 159, 85–111.

Schönfeld, J., Zahn, R., de Abreu, L., 2003. Surface and deep water response to rapid climate changes at the Western Iberian Margin. Glob. Planet Change 36, 237–264.

Shacketon, N.J., 2000. The 100,000-Year ice-age cycle identified and found to lag temperature, carbon dioxide, and orbital eccentricity. Science 289, 1897–1902.

Stuiver, M., Grootes, P.M., 2000. GISP2 oxygen isotope ratios. Quat. Res. 53, 277–284.

Telford, R.J., Andersson, C., Birks, H.J.B., Juggins, S., 2004. Biases in the estimation of transfer function prediction errors. Paleoceanography 19, PA4014 doi: 1029/2004PA001072.

Turon, J.-L., Lézine, A.-M., Denèfle, M., 2003. Land–sea correlations for the last glaciation inferred from a pollen and dinocyst record from the portuguese margin. Quat. Res. 59, 88–96.

Voelker, A.H.L., de Abreu, L., 2011. A review of abrupt climate change events in the northeastern Atlantic ocean (Iberian margin): latitudinal, longitudinal and vertical gradients. In: Rashid, H., Polyak, L., Mosley-Thompson, E. (Eds.), Abrupt Climate Change: Mechanisms, Patterns, and Impacts. AGU, Washington D.C, pp. 15–37.

Voelker, A.H.L., de Abreu, L., Schönfeld, J., Erlenkeuser, H., Abrantes, F., 2009. Hydrographic conditions along the Western Iberian Margin during Marine isotope Stage 2. Geochem. Geophys. Geosyst 10, Q12U08. http://dx.doi.org/10.1029/2009GC002605.

Voelker, A.H.L., Lebreiro, S.M., Schonfeld, J., Cacho, I., Erlenkeuser, H., Abrantes, F., 2006. Mediterranean outflow strengthening during northern hemisphere coolings: a salt source for the glacial Atlantic? Earth Planet. Sci. Lett. 245, 39–55.